European Conference on Computational Fluid Dynamics
ECCOMAS CFD 2006
P. Wesseling, E. Oñate and J. Périaux (Eds)
© TU Delft, The Netherlands, 2006

TOWARDS INTERACTIVE INDOOR THERMAL COMFORT SIMULATION

Christoph van Treeck[*],
Petra Wenisch[*], **André Borrmann**[*], **Michael Pfaffinger**[*], **Martin Egger**[*],
Oliver Wenisch[†] **and Ernst Rank**[*]

[*] Computational Civil and Environmental Engineering, Technische Universität München
Arcisstrasse 21, 80290 München, Germany
e-mail: treeck@bv.tum.de
web page: http://www.inf.bv.tum.de
[†]Leibniz Computing Centre of the Bavarian Academy of Sciences and Humanities,
Boltzmannstrasse 1, 85748 Garching, Germany
web page: http://www.lrz.de

Key words: Computational steering, fluid dynamics, grid generation, high performance computing, lattice Boltzmann methods, thermal comfort, turbulent convection.

Abstract. *The paper addresses the current state of the development of a computational steering environment (CSE) for interactive indoor thermal comfort simulation by utilizing high-performance supercomputing facilities. The CSE consists of a parallel CFD kernel, a fast spacetree-based 3D mesh generator and an integrated virtual reality-based visualization engine. The numerical method is based on a hybrid thermal lattice Boltzmann (LB) method with extensions for large eddy simulations of turbulent convective flows. We use a multiple-relaxation-time LB scheme for solving the mass and momentum equations numerically and a finite difference scheme for the heat equation. The CSE allows for modifying both the geometric model and the boundary conditions during runtime with immediate visualization of changes in the results. The application is demonstrated by two industrial applications with complex geometries, turbulent natural convection in the separator room of a ferry boat and turbulent convection in a train's passenger carriage. We currently enhance our model using a radiosity method with a fast spacetree-based visibility check and integrate a new local thermal comfort model developed by our partners.*

1 INTRODUCTION

Thermal comfort studies are of importance in several areas of application such as vehicles, train carriages and aircraft passenger cabins, buildings and machine rooms. The application of computational fluid dynamics (CFD) simulation tools is a state-of-the-art procedure employed in today's design process in order to predict system behaviour, reduce design cycles and further optimize products. Limited by the complexity of mesh generation and set-up of a numerical model, the application of these tools is restricted to a few parameter studies without changing the entire layout in each case. The form and layout definition of a product is mainly built upon the experience of the designing engineer.

In order to improve this situation, the tools presented in this paper allow for modifying both the geometric model and the boundary conditions during the runtime of a simulation with *immediate* visualization of changes in the results. This technique facilitates product optimization by studying the consequences of modified design parameters online. For given configurations further simulations can be posted as batch jobs for detailed studies in non-interactive mode using enhanced physical models at increased spatial resolution.

We emphasize the design and current status of the implementation of a computational steering environment (CSE), i.e. an interactive CFD environment allowing for local thermal comfort analysis by utilizing high-performance supercomputing facilities and virtual reality techniques. In particular, the interaction of the following components within an integrated environment is presented here: a parallel CFD code based on the hybrid thermal lattice Boltzmann method [15] using a multiple-relaxation-time scheme [6] with extensions for large eddy simulations of turbulent convective flows [31], a fast spacetree-based 3D mesh generator [33] and an interactive computational steering system with integrated VR-based visualization [32].

The CSE developments are the result of several research projects [33] and the long-term cooperation with our industrial partner SIEMENS AG, Corporate Technology. In order to overcome the classical evaluation of thermal comfort criteria for the human body as a whole, the scope of our current work within the COMFSIM research project [30] covers the development of a new, local thermal comfort model in conjunction with one of our partners, the Fraunhofer-Institute for Building Physics (Holzkirchen, Germany) and its integration into our simulation environment.

2 NUMERICAL METHOD

In the designated field of application – turbulent convective indoor air-flow simulation of non-reactive Boussinesq-incompressible Newtonian fluids – the mathematical model of the physical problem can be described by the set of five partial differential equations, the incompressible Navier-Stokes equations and the energy equation. As the buoyant nature of the flow can be modeled by the Boussinesq approximation, it is sufficient in this context to consider a coupling between the flow and the temperature field by a body force term accordingly.

The numerical method for solving the flow field is based on the lattice Boltzmann method (LBM), an efficient method for solving various fluid-flow problems [6, 14, 15, 24, 29]. In contrast to classical numerical methods LBM represent a bottom-up approach that emerged from lattice gas cellular automata. Utilizing methods of statistical physics, LBM compute the advection and local collision of an ensemble of particle distribution functions with respect to the Boltzmann equation with linearized collision operator [1, 14, 35].

2.1 Lattice Boltzmann method

The multiple relaxation time (MRT) lattice Boltzmann scheme proposed by d'Humières et al. [6] is used for the flow part. The advantage of this model over the popular single relaxation time model proposed by Bhatnagar, Gross and Krook (BGK model) [1] is its improved numerical stability which leads to a reduction in the oscillations in the pressure field. However, we observed that, if a turbulence model is applied, these oscillations may also be stabilized due to the damping effects of the introduced turbulent viscosity. The MRT scheme is based on a transformation of the discretized particle distribution functions from the phase space $\mathbb{F} = \mathbb{R}^B$ into a physically equivalent moment space $\mathbb{M} = \mathbb{R}^B$, where B is the number of discrete velocities in the model, which makes it possible to choose the relaxation parameters relating to the kinetic modes individually.

If we define the phase space by a set of $B = 15$ distribution functions $\{f_i(t, \vec{x}) : i = 0, ..., 14\}$ that evolve on a three-dimensional lattice corresponding to the velocity vectors $\{\vec{\xi}_i : i = 0, ..., 14\}$ in the settings of the D3Q15 model [24], the lattice Boltzmann evolution equation is written as

$$\vec{f}(t + \Delta t, \vec{x} + \vec{\xi}_i \Delta t) \; - \; \vec{f}(t, \vec{x}) \; = \; - \, \mathbf{M}^{-1} \, \hat{\mathbf{S}} \big[\vec{m}(t, \vec{x}) - \vec{m}^{(0)}(t, \vec{x}) \big] \quad . \tag{1}$$

With the matrix $\mathbf{M}$ given in ref. [6] a vector $\vec{f}$ in discrete velocity space is linearly mapped to a vector $\vec{f}$ in moment space, $\vec{m} = \mathbf{M}\, \vec{f}$, and vice versa, using the inverse $\mathbf{M}^{-1}$. We refer to [6, 14] for the optimum choice of relaxation coefficients s_i with $0 \leq s_i < 2$ of the collision matrix $\hat{\mathbf{S}} = diag(s_0, s_1, ..., s_{14})$ with respect to stability and dispersion properties. The kinetic moments for the 15-velocity model are

$$\vec{m} \; = \; (\rho, e, \varepsilon, j_x, q_x, j_y, q_y, j_z, q_z, 3p_{xx}, p_{ww}, p_{xy}, p_{yz}, p_{zx}, m_{xyz})^T \quad , \tag{2}$$

where density ρ and momentum $\vec{j}$ are conserved quantities and heat flux $\vec{q}$, stresses $(3p_{xx}, p_{ww}, p_{xy}, p_{yz}, p_{zx})$ and m_{xyz} are kinetic moments which are relaxed towards their equilibria $m_i^{(0)}(t, \vec{x})$. The latter are given in [6, 13].

We point out that the lattice Boltzmann equation (1) is obtained by discretizing the discrete Boltzmann equation – discrete in velocity space – by a first-order finite difference scheme in space and time. Alternatively, the discrete Boltzmann equation may be numerically treated in different ways, such as applying discontinuous Galerkin methods, see [8], or finite volume based schemes, for example.

However, it can be shown that the athermal lattice Boltzmann equation (LBE) scheme does not posses numerical viscosity, allows for high local element Reynolds numbers and yields quadratic convergence if appropriate boundary conditions are applied (see [11] for example) while the first order discretization scheme of the microscopic velocity space yields second order accuracy in space and time with respect to the macroscopic moments [14] if the low Mach number and low Knudsen number constraints are fulfilled [31]. Furthermore, the method can be efficiently implemented on high-performance computer hardware since the simple evolution scheme offers potential for optimization using vector pipelines, as demonstrated by the authors in [32].

2.2 Hybrid thermal model

As thermal lattice Boltzmann models (e.g. [28]) are hampered by numerical instabilities [15], we apply the hybrid thermal model according to the work of Lallemand and Luo [15] for simulating convective flows which we further extended by a large-eddy approach [31].

The conservation of mass and momentum is thereby decoupled from the energy conservation. A finite-difference discretization scheme was implemented to solve the diffusion-advection equation. Both numerical methods use the same underlying, uniform Cartesian grid with appropriate interpolation schemes at the boundaries [31]. The coupling between the athermal LBE and the finite difference scheme is explicit, i.e. the solution of the energy equation is used to compute a buoyant force

$$F_z(\vec{x}, t) \;=\; g_z \beta \, \Delta t \, T(\vec{x}, t) \tag{3}$$

in the sense of a Boussinesq approximation [29]. Thereby β is the thermal expansion coefficient, g_z is the acceleration due to gravity and the dimensionless temperature $T(\vec{x}, t)$ is scaled within the interval $[-1; +1]$. As mentioned in [15], a coupling to a second order moment must also be considered in order to obtain correct hydrodynamic equations. The temperature field is computed by means of the explicit scheme

$$\frac{1}{\Delta t^{FD}} \left(T_{i,j,k}(t + \Delta t^{FD}) - T_{i,j,k}(t) \right) \;=\; -\vec{j}_{i,j,k}(t) \boldsymbol{\nabla}^{(h)}_{i,j,k} T_{i,j,k}(t) \;+\; \alpha \boldsymbol{\Delta}^{(h)}_{i,j,k} T_{i,j,k}(t) \tag{4}$$

with the thermal diffusivity α and using adjusted time steps for the LBE and the FD part, as described by the first author in [31]. In order to avoid numerical instabilities, we use difference stencils with the same symmetry as for the phase space discretization, i.e. we use a 15-point stencil according to [15] for computing the operators $\boldsymbol{\nabla}^{(h)}_{i,j,k}$ and $\boldsymbol{\Delta}^{(h)}_{i,j,k}$.

We wish to point out that the low Mach number constraint requires that the chosen product $g_z \beta$ is sufficiently small; furthermore, the kinematic viscosity ν also has to fulfil the stability constraints of the MRT scheme, as there are restrictions on choosing the time step size Δt^{FD}. For details, see [15] and [31].

2.3 Extensions for LES

As opposed to the BGK model [1], the MRT scheme [6, 14] involves some computational overhead but increases numerical stability. Because in the MRT model the components of the traceless stress tensor are available locally as nodal quantities, it is straightforward to compute an eddy viscosity required for algebraic turbulence modeling [12, 13, 27, 31]. There is therefore no need to explicitly compute the stress or strain tensor by calculating derivatives of the (previously computed) velocity field. Algebraic closure models may be applied if the subgrid scale is assumed to be homogenous and isotropic; near walls the subgrid stresses should tend towards zero.

Besides numerical issues, the analysis of local thermal comfort requires a knowledge of the transient turbulent nature of a flow field, for example, the degree of turbulence.

As these effects are damped by models based on the Reynolds averaged Navier-Stokes equations (RANS models), we favour large-eddy simulation (LES) with implicit filtering over the explicit modeling of all scales of the turbulent kinetic spectrum.

LES solves the Navier-Stokes equations in a volume-averaged manner where small unresolved scales are suppressed by filtering techniques, which causes additional subgrid scale stresses. The deviatoric part of these stresses is modeled whereas large-scale eddies, which possess most of the turbulent kinetic energy in the system, are resolved by the numerical scheme. In the Smagorinsky model [26], these dissipative effects are interpreted as eddy viscosity ν_T which is related to the strain rate

$$\widetilde{\epsilon}_{\alpha\beta} = \frac{1}{2}(\frac{\partial u_\alpha}{\partial x_\beta} + \frac{\partial u_\beta}{\partial x_\alpha}) \tag{5}$$

by

$$\nu_T \;=\; C_s^2 \Delta^2 \, |\widetilde{\epsilon}_{\alpha\beta}| \tag{6}$$

where C_s is the Smagorinsky constant and the filter width is given by $\Delta = (\Delta x \Delta y \Delta z)^{1/3}$. We refer to [3] for a review of the appropriate choice of parameters. As shown in [12, 13, 31], within the scope of lattice Boltzmann methods, the local strain tensor can be obtained from the momentum flux tensor, i.e. the second-order moments of the distribution functions which are given as local quantities.

The turbulent stresses are accordingly combined with the molecular viscosity ν_0 to form a total viscosity $\nu_{total} = \nu_0 + \nu_T$, which replaces the material property ν by a space and time dependent quantity. In our explicit scheme, we relate new values for ν_T to the time step before advection takes place to obtain the relaxation parameters for the second order moments related to stress, as shown in [29].

Neglecting viscous dissipation, we model the subgrid scale heat flux

$$\widetilde{q}_i^{sgs} \;=\; \lambda_T \, \frac{\partial \widetilde{T}}{\partial x_i} \;=\; \rho c_p \alpha_T \, \frac{\partial \widetilde{T}}{\partial x_i} \tag{7}$$

using an eddy diffusivity approach in the volume-averaged, incompressible heat equation

$$\rho c_p \frac{\partial \widetilde{T}}{\partial t} + \rho c_p \, \widetilde{u}_i \frac{\partial \widetilde{T}}{\partial x_i} \;=\; -\frac{\partial}{\partial x_i}\big(\, \widetilde{q}_i^{mol} \;+\; \widetilde{q}_i^{sgs} \,\big) \quad , \tag{8}$$

with $\widetilde{q}_i^{mol} = -\lambda \, (\partial \widetilde{T} / \partial x_i)$, the heat conductance of the fluid λ and the specific heat capacity at constant pressure c_p. The turbulent viscosity and the turbulent heat diffusivity α_T are correlated at each lattice site by the turbulent Prandtl number, which is assumed to be constant in the core domain [25].

Our thermal code is validated in 2D and 3D for laminar and turbulent natural convection at various Rayleigh numbers. A discussion of Nusselt number correlations and a comparison to benchmark data is given in [29] and [31].

3 FAST SPACE-TREE BASED DISCRETIZATION

Fast, fully automated grid generation capabilities are essentially required for supporting interactive CFD sessions with immediate updates in sub-second time frames. Interactivity means inserting, removing, translating, transforming, rotating and scaling of geometric objects during simulation as well as modifying boundary conditions.

As indicated in the last section, both numerical schemes use the same uniform Cartesian grid. For discretization, a space-tree based partitioning algorithm was implemented [34]. The serial version of the grid generator software allows for meshing arbitrarily shaped, complex facette models within fractions of up to a few seconds computing time (see also next section for an example). In order to improve its performance still further, the algorithm is parallelized using OpenMP. It is referred to [32] for speed-up measurements.

By enclosing geometrical objects with a cubic bounding box, the algorithm is continued by recursively dividing this cube into eight sub-cubes with half edge-length as long as a cube intersects with the geometry or until a given resolution, i.e. a minimum edge length h, is reached. An octree of depth t therefore approximates a domain with the resolution $h = \mathcal{O}(2^{-t})$. Voxels are identified as being inside, outside or at the boundary of a geometric object. In order to support space interpolation schemes, voxels are linked to facets and the distances along the directions of the microscopic velocity vectors are evaluated at the boundaries.

For example, the serial discretization up to level 7 (29,500 voxels) of a facetted object with 30,000 triangles takes 0.67 seconds on a normal desktop PC. We wish to point out that the algorithm does not fail if the model is geometrically inconsistent, i.e. if there are small gaps between facets. Please refer to [29, 32, 34] for further details.

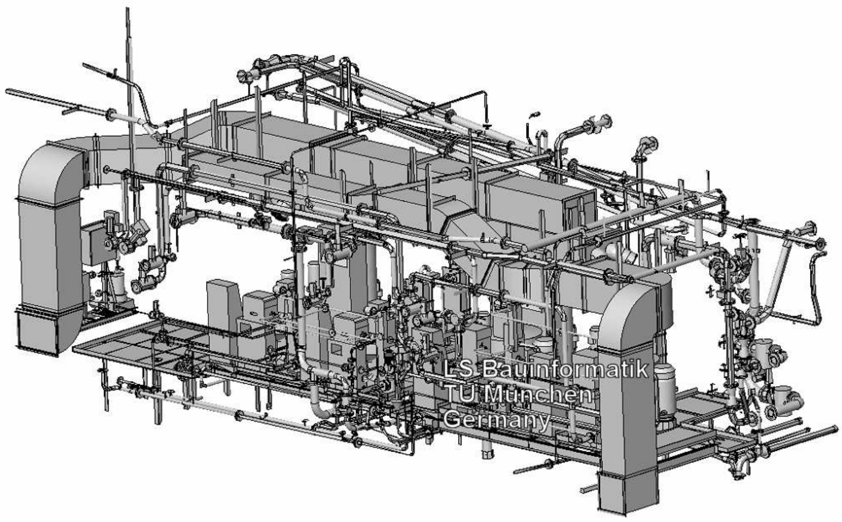

Figure 1: Geometric model of separator room of ferry boat (part of engine system). The model consists of 295,899 facets. Courtesy of Flensburger Schiffsbaugesellschaft (FSG), Germany.

4 APPLICATION A: SEPARATOR ROOM IN A FERRY BOAT

In this section we demonstrate the application of our grid generator software and our parallel thermal code. Figure 1 shows the geometric model of the separator room of a ferry boat which is part of the engine system. The facette model was obtained from a CAD system and consists of 295,899 triangles. The interface of our software supports the stereo lithography (STL) file format which is common to most CAD systems. The computing time for the whole model discretization with 1.5 million grid points on a $200 \times 75 \times 100$ grid took 3,7 seconds in serial mode (without file I/O).

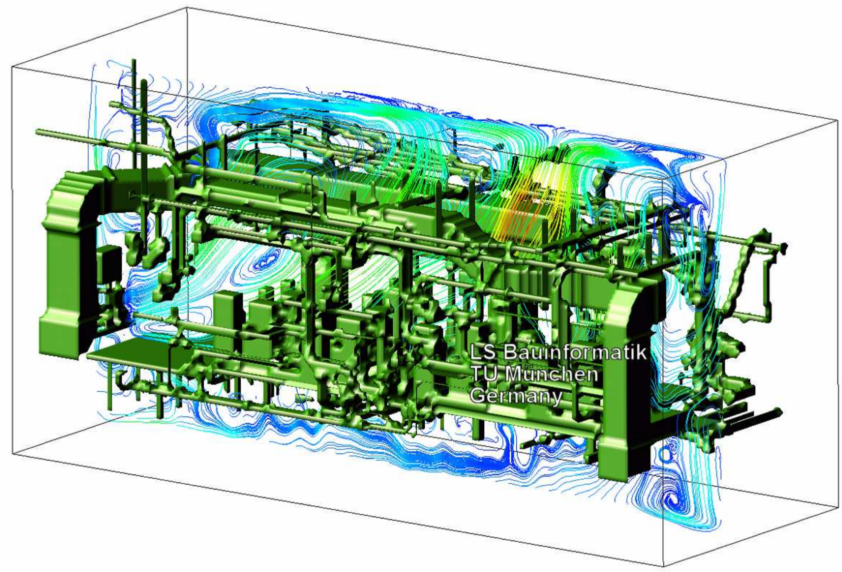

Figure 2: Turbulent natural convection in separator room of ferry boat (part of engine system). Four hot devices located midway have to be air cooled in order to satisfy working condition requirements. Courtesy of Flensburger Schiffsbaugesellschaft (FSG), Germany.

The lattice Boltzmann simulation (24 million degrees of freedom) was performed on a parallel AMD Opteron linux cluster for the physical problem of $Ra \approx 10^{10}$ and $Pr = 0.71$ using 80 CPUs within a few hours computing time. Figure 2 shows streamlines of the averaged velocity field in a vertical plane, red (blue) colors indicate high (low) temperature values. Four hot separator devices located midway have to be air cooled in order to satisfy working condition requirements.

As the pilot study primarily aimed at demonstrating the potential of LBM for industrial purposes, we would mention that the whole process from data delivery, model setup, grid generation and simulation up to an initial postprocessing, as demonstrated in the figures, was performed within a single working day. This is generally achieved by the fast grid generation techniques applied. It was neither necessary to reduce the model's level of detail nor to explicitly check the model for inconsistencies, such as small gaps between facets, due to modeling inaccuracies or rounding-off errors caused by geometrical transformations.

5 COMPUTATIONAL STEERING ENVIRONMENT (CSE)

Computational steering means 'interacting with the simulation itself' [32]. It is therefore more than adopting the serial (or batch) sequence of operations covering the preprocessing, simulation and postprocessing stages and its iterative repetition with modifications in parameters or confining oneself to 'interactive postprocessing' or 'visualization on the fly' only. The term is unfortunately often misunderstood as some kind of process monitoring. As stated in [22], computational steering "enables scientists to directly change parameters of the simulation process during execution and to analyze the effects of these interactions immediately".

As indicated in Section 3, we use the term interactivity to mean modifying boundary conditions as well as inserting, removing, translating, transforming, rotating and scaling of geometric objects (e.g. active components such as heaters or passive fluid obstacles) during simulation. In our CSE, users may start from scratch or load predefined environments such as a passenger cabin scenario and add further components during simulation. These features and the inherent flexibility are not known to the authors in other CSE systems. A review of recent developments in the field of computational steering is given by the authors in [32].

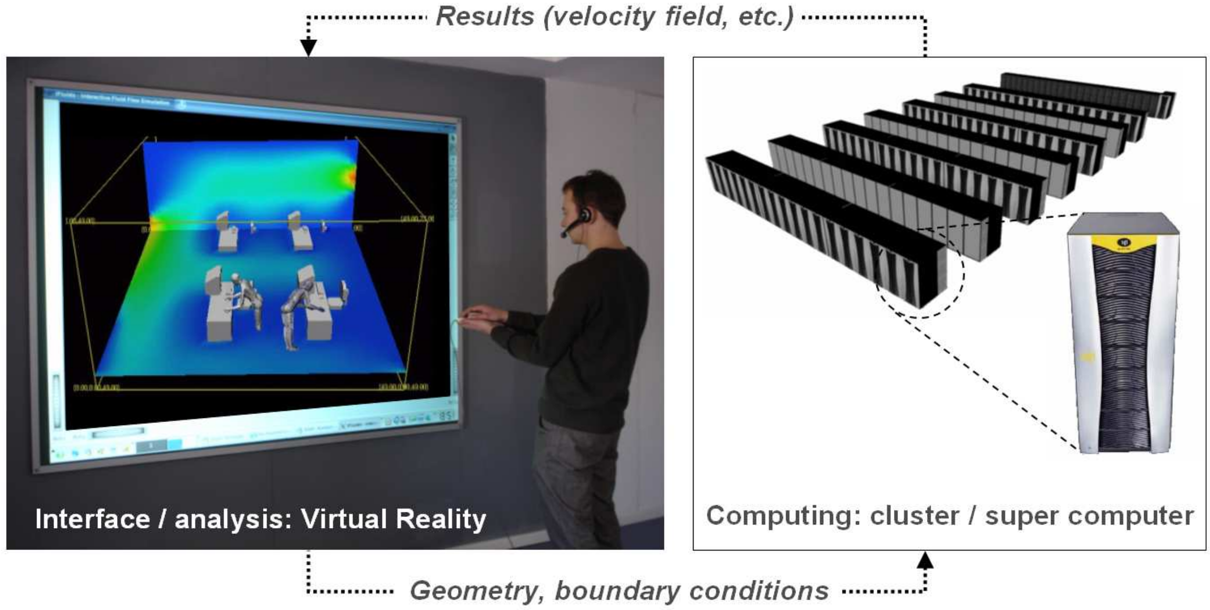

Figure 3: Basic principle of computational steering. The picture on the left-hand side shows our stereoscopic visualization system (rear projection). Modifications of the geometry are communicated to the supercomputer which updates the velocity/temperature fields. On the right-hand side the layout of the new German national supercomputer HLRB-II [23] is displayed (33 TFlop/s in 2006, 69 TFlop/s in 2007).

Figure 3 shows the basic principle of our CSE by demonstrating an online session using our institute's stereoscopic visualization facilities. Modifications of the geometry are communicated to the supercomputer, which immediately updates the velocity/temperature fields accordingly.

Our modular CSE [32, 33, 34] consists of

- a fast spacetree based 3D mesh generator (cf. Section 3),
- an integrated virtual reality-based visualization engine supporting various hardware devices such as common desktop displays, passive and active stereoscopic visualization devices,
- an efficient short-latency communication interface between kernel and visualization [33],
- extensions supporting collaborative engineering applications where multiple visualization clients may be attached or detached [2] and
- a parallel computing kernel that makes use of GRID capabilities supporting both an optimized athermal lattice BGK model [32] and the described MRT hybrid thermal lattice Boltzmann model [31], both with algebraic turbulence model extensions.

As can be seen from Figure 4, we integrated an interactive user interface with a context-based 3D menu to provide an intuitive front-end in the application. The picture on the left-hand side, for example, demonstrates the interaction with draggers to manipulate objects in the scenario of a passenger cabin while the flow field is illustrated using common

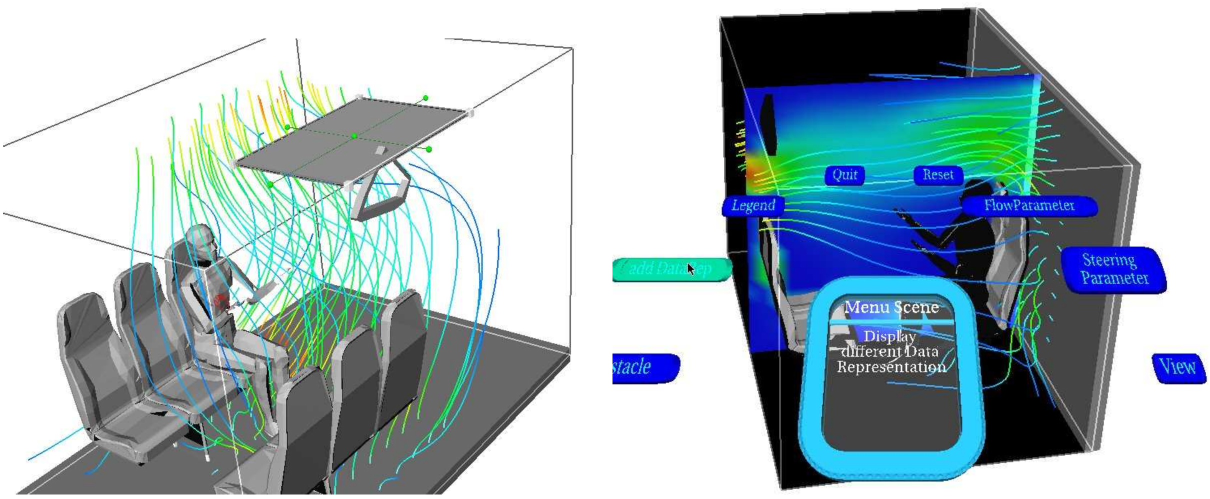

Figure 4: Screenshot of online interactive simulation run of air flow inside a passenger cabin. The right-hand side shows the menu of the integrated VR user interface.

techniques, for example, a streamline plot. This approach clearly allows engineers to design ventilation concepts, for example, with respect to choosing the optimum positions for inlets and outlets, respectively.

Our implementation makes use of the Mercury OpenInventor library [20] and supports VR environments with single or multiple projection screens and head/input device tracking. The event-driven communication concept is based on a simulation master node that interacts with a number of slave nodes. The inter-machine communication between computational steering (visualization) front-end and master node (supercomputer) is implemented using Globus MPICH-G2 [16] or PACX-MPI [17] while slave nodes mutually interact using vendor-optimized MPI libraries. We refer to [32] for a detailed description of the communication interface.

6 APPLICATION B: TRAIN PASSENGER CABIN

We extend the example introduced in the CSE section in Figure 4 and consider turbulent natural convection in the open carriage of a train. The buoyant flow is driven by two lines of heaters placed along the lower section of the seats next to the cabin walls. Figure 5 displays the visualization of the averaged velocity field within the whole passenger cabin while Figure 6 gives a more detailed view and shows the corresponding discrete voxel model.

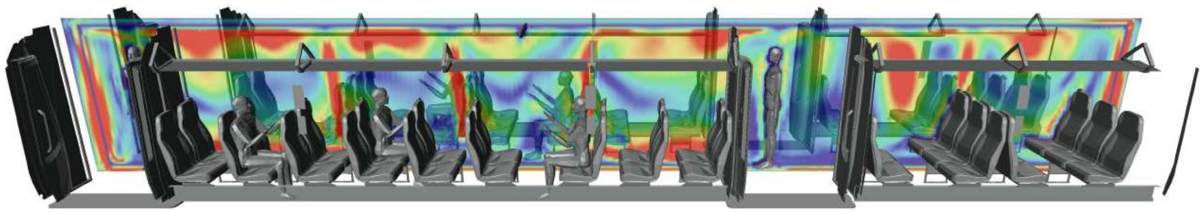

Figure 5: Turbulent convection in train passenger cabin. Visualization of the averaged velocity field. Red (blue) colors indicate high (low) flow velocities.

The simulation with 40 million degrees of freedom was performed on our parallel Opteron Cluster using 16 CPUs in a few hours computing time until a steady state solution was reached. The grid generation took about 1.5 seconds for the whole model. The study was performed in cooperation with SIEMENS AG, Corporate Technology.

7 THERMAL COMFORT STUDIES

The scope and purpose of internal air flow simulations, as depicted in Figures 5 and 6, is to provide an estimate of human comfort during the early design stages. Motivated by the work of P.O. Fanger, such as [9, 10], the European standard [7] gives formulae for computing a statistical measure of the thermal comfort level, which is quantified by indices that correlate physical values obtained by simulation. Input parameters are the

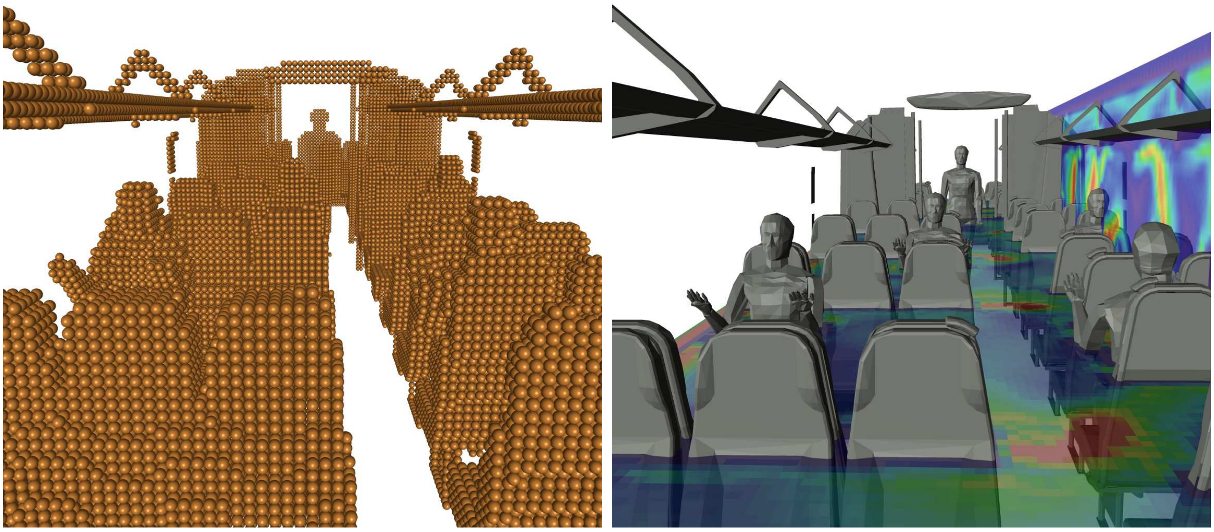

Figure 6: Turbulent convection in train passenger cabin. The left-hand picture shows the discrete voxel model, with the averaged velocity field portrayed on the right-hand side(40 million degrees of freedom).

individual's level of activity and clothing, the mean air temperature, the mean radiant temperature of surrounding surfaces, the relative humidity and the air velocity field with fluctuations in order to compute the degree of turbulence. The computation of the comfort indices for the predicted mean vote (PMV) and predicted percentage of dissatisfied

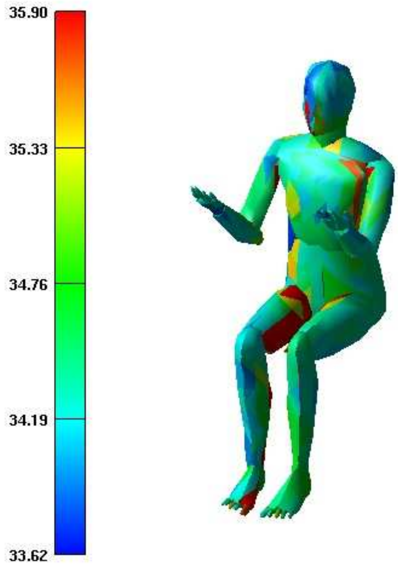

Figure 7: Computation of the resultant surface temperature (RST) [19] at the surface of the numerical dummy [4]. The RST serves as input for the local thermal comfort evaluation. Units are given in [$^{\circ}C$].

(PPD) is a state-of-the-art technique in the industrial context and has previously been demonstrated by the authors, for example in the scope of LBM in [5] or using a commercial solver coupled to a thermal multizone building model in [29].

The aforementioned models are based on the quantitative evaluation of the heat balance of a human body and its metabolism *as a whole*. Thereby the energy produced, i.e. the difference between metabolic rate and conducted mechanical work, is related to the energy emitted into the environment, i.e. energy transferred by convection, radiation and conduction through clothing as well as latent and respirative heat exchange [7, 9].

However, the aim of our current research is to integrate a new *local* model into our CFD system that transfers these well-established methods for evaluating the overall comfort level to dedicated parts of the body bearing local levels of clothing and activity in mind. This model is currently developed in the COMFSIM framework [30] by our partners, the Fraunhofer Institute for Building Physics (IBP) in Germany and is based on the work published in [18, 19].

We therefore developed a postprocessing prototype that computes resultant surface temperatures (RST), see [19], which are mapped to the (surface) facets of the surface of a numerical mannikin by assuming a constant heat flux emitted from its artificial skin, as depicted in Figure 7. Numerical results obtained from a LES simulation have been compared in a detailed study on measurement data in a testing facility provided by the IBP. The promising results of this study are given in [4]. We are currently integrating the module into our CSE for an online evaluation.

8 CONCLUSIONS AND OUTLOOK

In this paper, we have presented the status of our work on the development of an interactive computational steering environment for local thermal comfort analysis utilizing high-performance supercomputers. The numerical method is based on the hybrid thermal lattice Boltzmann model proposed by Lallemand and Luo [15] with extensions by a Smagorinsky subgrid scale model [31].

An aspect of the COMFSIM research project [30] currently under investigation involves the integration of a new local thermal comfort model being developed by our partners. In order to resolve all the physical quantities concerned, a module for computing short and long-wave radiative heat transfer is being implemented where the latter is based on the radiosity method with a fast visibility check utilizing space tree data structures and a level of detail-dependent view factor determination. We would refer to future publications.

Other ongoing work deals with optimizing our hybrid thermal code with respect to the new national supercomputer SGI Altix 4700 [23]. Currently, our system is aligned to the HITACHI SR8000-F1 system, a parallel pseudo-vector supercomputer [32, 33].

As the hybrid thermal model requires higher order boundary conditions [15, 21, 31], we are investigating these schemes from the point of view of the general facette model applied in the discretization process. As regards computational steering issues, this approach involves the use of most efficient data structures and communication concepts, since the data locality inherent to LBE schemes that use the standard bounce-back algorithm is violated. We thereby anticipate some substantial benefits from the new computer which is characterized by a shared memory architecture with cache-coherent non-uniform memory access (ccNUMA).

9 ACKNOWLEDGEMENTS

The authors are grateful to the Bayerische Forschungsstiftung (Munich, Germany), KONWIHR (Competence Network for Technical Scientific High Performance Computing in Bavaria, Germany) and to the SIEMENS AG, Corporate Technology for financial support. Part of this work is being sponsored by grant No. AZ 630/04 awarded by the Bayerische Forschungsstiftung. The results presented in this paper form part of the work being undertaken within the research project COMFSIM and ViSimLab. The authors would like to thank the Flensburger Schiffsbaugesellschaft for valuable discussions and for providing the geometrical data depicted in Figures 1 and 2.

REFERENCES

[1] P. Bhatnagar, E.P. Gross, and M.K. Krook. A model for collision processes in gases. *Physical Review*, 94(3):511–525, 1954.

[2] A. Borrmann, P. Wenisch, C. van Treeck, and Rank E. The collaborative computational steering platform CoCoS: Principles and application in collaborative hvac layout using interactive fluid simulations. *Integrated Computer-Aided Engineering (ICAE)*, submitted, 2005.

[3] M. Breuer. *Direkte numerische Simulation und Large-Eddy Simulation turbulenter Strömungen auf Hochleistungsrechnern.* Professorial dissertation, Lehrstuhl für Strömungsmechanik, Friedrich-Alexander-Universität Erlangen-Nürnberg, 2001.

[4] N. Cenic. *Development of thermal comfort temperature sensors using CFD simulation based on lattice Boltzmann methods.* Master thesis, TU Munich, 2005.

[5] B. Crouse, M. Krafczyk, S. Kühner, E. Rank, and C. van Treeck. Indoor air flow analysis based on lattice boltzmann methods. *Int. J. Energy and Buildings*, 34(9):941–949, 2002.

[6] D. d'Humières, I. Ginzburg, M. Krafczyk, P. Lallemand, and L.-S. Luo. Multiple-relaxation-time lattice Boltzmann models in three dimensions. *Phil. Trans. R. Soc. Lond. A*, 360:437–451, 2002.

[7] DIN EN ISO 7730. *Analytische Bestimmung und Interpretation der thermischen Behaglichkeit durch Berechnung des PMV- und des PPD-Indexes und der lokalen thermischen Behaglichkeit.* DIN Deutsches Institut für Normung e.V., Beuth, 2003.

[8] A. Düster, L. Demkowicz, and E. Rank. High-order finite elements applied to the discrete Boltzmann equation. *Int. J. for Num. Meth. in Eng.*, in press, 2006.

[9] P.O. Fanger. *Thermal comfort.* Robert E. Krieger, Malabar, 1982.

[10] P.O. Fanger, J. Ostergaard, O. Olesen, T. Madsen, and Lund. The effect on man's comfort of a uniform air flow from different directions. *ASHRAE Transactions*, 80:142–157, 1974.

[11] I. Ginzburg and D. d'Humières. Local second-order boundary methods for lattice Boltzmann models. *J. Stat. Phys.*, 84:927–971, 1996.

[12] S. Hou et al. A lattice-Boltzmann subgrid model for high Reynolds number flows. *Fields Inst. Comm.*, 6:151–165, 1996.

[13] M. Krafczyk, J. Tölke, and L.-S. Luo. Large-eddy simulations with a multiple-relaxation-time LBE-model. *Int. J. Modern Physics B*, 17:33–39, 2003.

[14] P. Lallemand and L.-S. Luo. Theory of the lattice Boltzmann method: Dispersion, dissipation, isotropy, Galilean invariance, and stability. *Physical Review E*, 61(6):6546–6562, 1999.

[15] P. Lallemand and L.-S. Luo. Theory of the lattice Boltzmann method: Acoustic and thermal properties in two and three dimensions. *Physical Review E*, 68(036706), 2003.

[16] MPICH-G2 library, 2006. http://www3.niu.edu/mpi.

[17] PACX-MPI library, 2006. http://www.hlrs.de/organization/pds/projects/pacx-mpi.

[18] E. Mayer. A new correlation between predicted mean votes (PMV) and predicted percentages of dissatisfied (PPD). In *Healthy Buildings/IAQ'97*, pages 189–193, Washington DC, 1997.

[19] E. Mayer. Manfitted measurement of thermal climate by a dummy representing suit for simulation of human heatloss (DRESSMAN). In *Healthy Buildings*, volume 2, pages 551–556, Washington DC, 2000.

[20] Mercury. OpenInventor library, 2006. http://www.tgs.com.

[21] A. Mezrhab, M. Bouzidi, and P. Lallemand. Hybrid lattice-Boltzmann finite-difference simulation of convective flows. *Computers and Fluids*, 33:623–641, 2004.

[22] J. D. Mulder, J. J. van Wijk, and R. van Liere. A survey of computational steering environments. *Future Gener. Comput. Syst.*, 15(1):119–129, 1999.

[23] Leibniz Computing Centre of the Bavarian Academy of Sciences and Humanities, 2006. http://www.lrz-muenchen.de.

[24] Y.H. Quian, D. d'Humières, and P. Lallemand. Lattice BGK models for Navier-Stokes equations. *Europhys. Lett.*, 17(6):479–484, 1992.

[25] H. Schlichting and K. Gersten. *Boundary layer theory.* Springer, 9. edition, 1996.

[26] J. Smagorinsky. General circulation experiments with the primitive equations, I, The basic experiment. *Mon. Weather Rev.*, 91:99–165, 1963.

[27] C.M. Teixeira. Incorporating turbulence models into the lattice-Boltzmann method. *Int. J. Modern Physics C*, 9(8):1159–1175, 1998.

[28] G. Vahala, P. Pavlo, L. Vahala, and N.S. Martys. Thermal lattice-Boltzmann models (TLBM) for compressible flows. *Int. J. Modern Physics C*, 9(8):1247–1261, 1998.

[29] C. van Treeck. *Gebäudemodell-basierte Simulation von Raumluftströmungen.* PhD thesis, Technical University Munich, 2004.

[30] C. van Treeck and E. Rank. ComfSim - Interaktive Strömungssimulation und lokale Komfortanalyse in Innenräumen. In Bayerische Forschungsstiftung, editor, *Jahresbericht 2005*, page 66, München, Germany, 2006.

[31] C. van Treeck, E. Rank, M. Krafczyk, J. Tölke, and B. Nachtwey. Extension of a hybrid thermal lbe scheme for Large-Eddy simulations of turbulent convective flows. *Computers and Fluids*, in press, 2005.

[32] P. Wenisch, C. van Treeck, A. Borrmann, E. Rank, and O. Wenisch. Computational steering on distributed systems: indoor comfort simulations as a case study of interactive CFD on supercomputers. *Int. J. Parallel, Emergent and Distributed Systems*, submitted, 2006.

[33] P. Wenisch, C. van Treeck, and E. Rank. Interactive indoor air flow analysis using high performance computing and virtual reality techniques. In *Roomvent Conference*, Portugal, 2004.

[34] P. Wenisch and O. Wenisch. Fast octree-based voxelization of 3D boundary representation objects. Technical report, Lehrstuhl für Bauinformatik, Technische Universität München, 2004.

[35] G. Zanetti and McNamara. Use of the boltzmann equation to simulate lattice-gas automata. *Phys. Rev. Lett.*, 61:2332–2335, 1998.